

Highly Transparent Nanostructured Zinc Oxide Photodetector Prepared by Successive Ionic Layer Adsorption and Reaction

Pay-Yu Lee¹, Sheng-Po Chang^{*1}, Jui-Fu Chang², En-Hao Hsu², Shoou-Jinn Chang¹

¹Institute of Microelectronics & Department of Electrical Engineering, Center for Micro/Nano Science and Technology, Advanced Optoelectronic Technology Center, National Cheng Kung University, Tainan 70101, Taiwan

²Department of Electrical Engineering, National University of Tainan, 700 Taiwan

*E-mail: changsp@mail.ncku.edu.tw

Received: 27 March 2013 / Accepted: 15 April 2013 / Published: 1 May 2013

We report for the first time the fabrication of a ZnO PD by SILAR involving the use of ethylene glycol. The average diameter of ZnO was around 100 nm. In addition, the obtained hexagonal ZnO thin films grew along the c-axis and with stronger intensity at the peak (002) plane; further, the films had a smooth surface morphology and showed high transparency in the visible spectral range. The fabricated ZnO PD was visible-blind with a cutoff wavelength around 350 nm. Under a 10 V applied bias, the measured dark current was 2.58 μ A and the photocurrent was 803 μ A, and hence, the responsivities were 68.5 A/W for the ZnO PD.

Keywords: ZnO, SILAR, Ethylene glycol, Photodetector, Thin films

1. INTRODUCTION

ZnO is an important semiconductor material with a large bandgap ($E_g = 3.37$ eV) that crystallizes in the hexagonal wurtzite structure ($c = 0.521$ nm, $a = b = 0.325$ nm), with oxygen and zinc atoms occupying hexagonal and tetrahedral sites, respectively. ZnO also has high stability, good optical characteristics, and excellent electrical properties. ZnO thin films have been widely used in various devices such as piezoelectric transducers, surface acoustic wave filters, thin-film solar cells, gas sensor electronics, and ultraviolet (UV)-light-emitting diodes. In addition, ZnO films with high transmittance in the visible region and low resistivity are suitable for use as transparent electrodes in electronic displays. ZnO thin films have been prepared by various chemical and physical deposition techniques such as sputtering, pulsed laser ablation, successive ionic layer adsorption and reaction

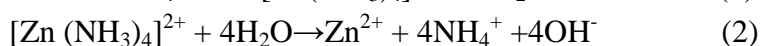
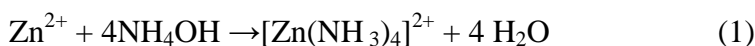
(SILAR) [1–10], sol-gel methods [11–13], chemical bath deposition (CBD) [14–16], and chemical vapor deposition (CVD) [17]. Among these, solution-based chemical deposition techniques (e.g., SILAR) have recently attracted considerable attention because they are highly reliable and inexpensive; furthermore, these methods require low temperatures and facilitate large-area deposition, as opposed to other methods. However, very less effort has been devoted to the fabrication of transparent ZnO films via SILAR.

Recently, Gao *et al.* [1] included an ultrasonic rinsing step in the SILAR process for the preparation of ZnO thin films. SILAR is a simple and versatile method for thin film growth that allows for the easy deposition of films. It does not require high-quality substrates and can be performed at room temperature without the need for vacuum. Besides, it is cost-effective and can adapt to any substrate material (insoluble) or surface profile. Growth parameters are relatively easy to control, yielding stoichiometric deposits with tunable grain sizes. However, only a few publications describe the sensing behavior of the ZnO thin films deposited by aqueous solution techniques at low temperatures [3–5]. To the best of our knowledge, there are no reports on the fabrication of ZnO photodetectors by SILAR methods. In this study, we report for the first time the fabrication of ZnO photodetectors (PDs) by a SILAR method with ethylene glycol. The physical and electro-optical properties of the fabricated ZnO thin film PD are also discussed.

2. EXPERIMENTAL

ZnO thin films were grown on glass substrates by the SILAR method. In the experiments, 0.1 M ZnCl₂ and concentrated 29% ammonia (NH₄OH) solutions were used to prepare the zinc complex (Zn(NH₃)₄²⁺) precursor solution. NH₄OH was added to complex the Zn(II) ions and to buffer the solution pH to 10. For the growth of ZnO films, a 20-cycle deposition was carried out. Using the SILAR method to deposit ZnO thin films, we set the temperature of ethylene glycol at 125°C to convert Zn(OH)₂ to ZnO. The detailed procedures for preparing ZnO films in one cycle is described as follows: (i) the glass substrates were dipped in the zinc complex solution for 20 s; (ii) once Zn(OH)₂ precipitated on the substrates, the glass was dipped in deionized (DI) water for 20 s; (iii) the substrates were sonicated for 30 s in DI to remove the adsorbed Cl⁻ ions and loosely attached Zn(OH)₂ grains; (iv) the substrates were dipped in ethylene glycol solution and heated at 125 °C for 20 s to generate ZnO; (v) finally, the substrates were sonicated in DI for 30 s to remove excess ethylene glycol, loosely attached ZnO grains, and unreacted Zn(OH)₂ from the surface.

The chemical reactions occurring in the corresponding procedure are given in equations (1) to (4):



After the 20-cycle deposition, a series of ZnO thin film samples were deposited on glass. The structure and crystallite size of the films were investigated by X-ray diffraction (XRD). The surface morphologies of the samples were examined using scanning electron microscopy (SEM) and atomic force microscopy (AFM). The optical properties of the ZnO thin films were characterized by an ultraviolet-visible-near-infrared (UV-VIS-NIR) spectrophotometer.

To fabricate the ZnO UV PD, we deposited a thick Pt (100 nm) film through an interdigitated shadow mask onto the ZnO thin films to serve as the contact electrode. We designed the interdigitated shadow mask to be 2 mm wide and 2.2 mm long with a finger spacing of 0.2 mm. Current-voltage (I-V) characteristics of the fabricated PDs were then measured by an HP 4156 semiconductor parameter analyzer at room temperature. Spectral responsivity measurements of the PDs were also performed at room temperature by a JOBIN-YVON SPEX System with a 300-W Xe arc lamp light source (PERKINELMER PE300BUV) and a standard synchronous detection scheme.

3. RESULTS AND DISCUSSION

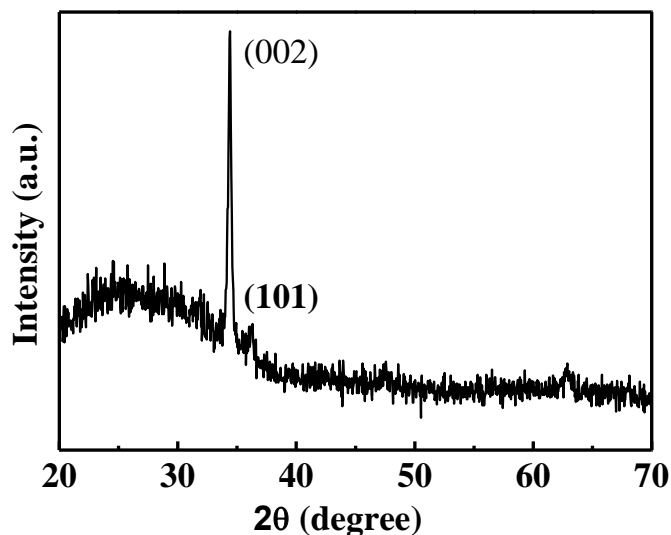


Figure 1. XRD analysis of ZnO thin film prepared by SILAR method.

Figure 1 shows the XRD patterns of ZnO thin films deposited at 125°C for 20 cycles. For the ZnO thin films, the highest peak corresponding to the (002) plane of wurtzite was located around the diffraction angle (2θ) of 34.42°; the strongest intensity of this diffraction peak indicated that the film grew along the c-axis. Figure 2(a) shows the SEM images for the surface of the ZnO thin films. The thin film surfaces were smooth and dense, with a particle size smaller than 100 nm. Figure 2(b) shows AFM images of the surface morphologies of the deposited ZnO films over a $2 \times 2 \mu\text{m}^2$ scan area. The root mean square (rms) value of the ZnO grain size in the film was 20.16 nm. The results revealed that the ZnO thin films had a smooth surface topology.

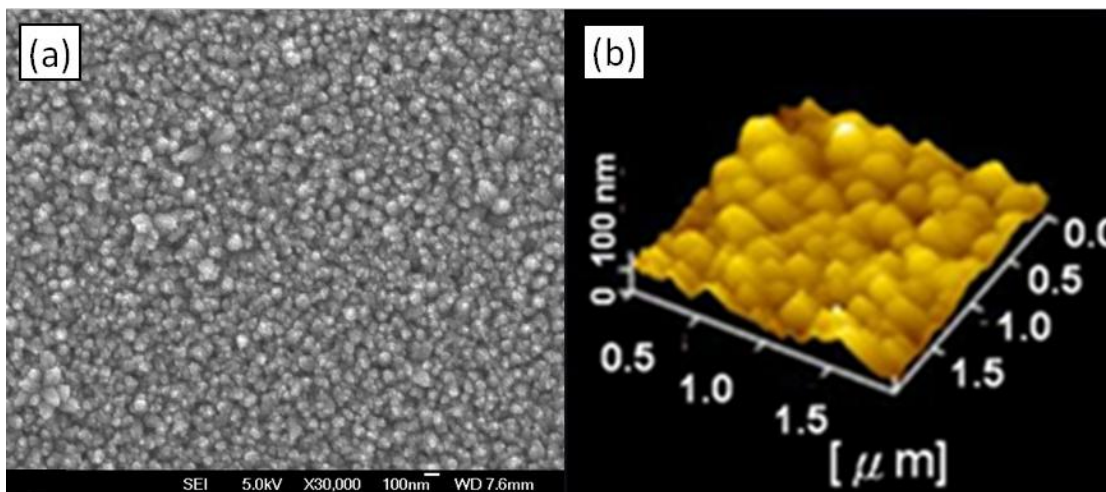


Figure 2. Top-view FE-SEM (a) and AFM (b) images of ZnO thin film.

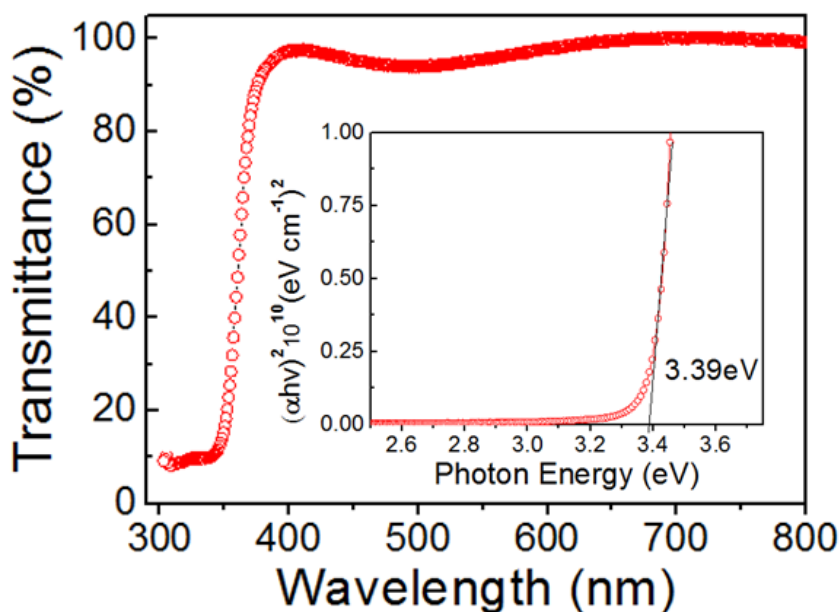


Figure 3. Optical transmittance spectra of the deposited ZnO films deposited at 125 °C. Inset: Plot of $(\alpha hv)^2$ as a function of incident light photon energy.

Figure 3 shows the optical transmittance spectra of the ZnO thin films, depicting that their optical transmittance was as high as 90% in the visible-light wavelength region. The sharp ultraviolet absorption edges were about 350 nm. The ZnO band gap was estimated by extrapolation of the linear portion of the α^2 versus $h\nu$ plots, using the relation $(\alpha hv)^2 = A(h\nu - E_g)$, where α is the absorption coefficient, $h\nu$ is the photon energy, and E_g is the optical band gap. The obtained ZnO thin films had a 3.39 eV bandgap, which was very close to the 3.37 eV band gap of ZnO.

Figure 4 shows the I-V characteristics of the fabricated ZnO thin film PD, in the dark and under UV illumination. During photocurrent measurements, we illuminated the sample with 350-nm UV light by dispersing a 300-W Xe arc lamp with a monochromator. With a 10 V bias, it was found that

dark currents measured 2.58 μA . Under the same conditions, the measured photocurrents increased to 803 μA .

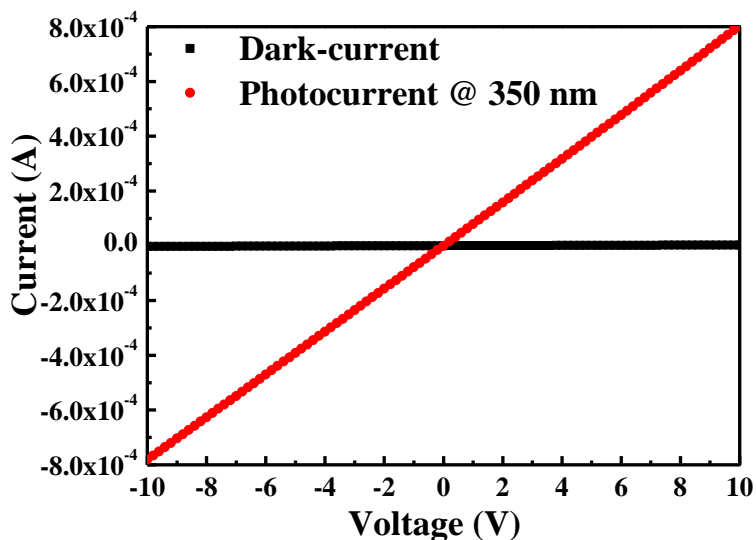


Figure 4. Room-temperature I-V characteristics of the ZnO thin film PD, measured in the dark (black squares) and under 350-nm UV illumination (red circles)

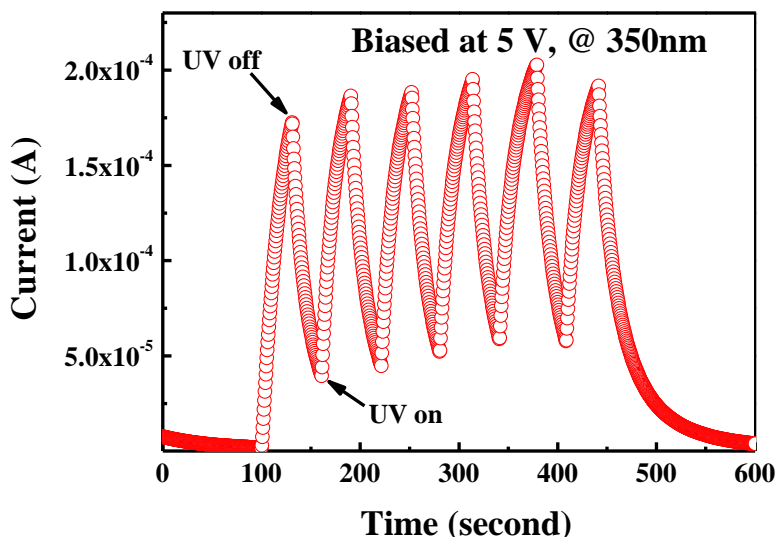


Figure 5. Photocurrent transient response of the fabricated ZnO thin film PD as the 350 nm-UV excitation was switched on and off. Film was biased at 5 V.

The significantly larger photocurrent also provides us a large photocurrent-to-dark current contrast ratio for the ZnO PD. Figure 5 shows the measured transient response of the fabricated ZnO PD, as we switched the UV excitation on and off every 25 s. It was found that the dynamic response of the ZnO PD was stable and reproducible with an on/off current contrast ratio of around 3 under 5 V

applied bias. It was also found that photocurrent first increased rapidly and then increased at a much lower rate as under UV excitation. A similar response was observed under the dark conditions.

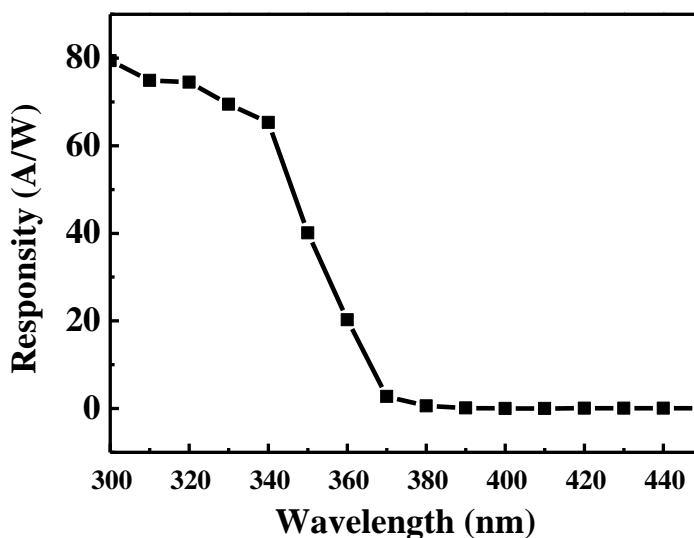


Figure 6. Room-temperature spectral responses of the ZnO thin film PDs measured with a 5 V applied bias.

Figure 6 shows the room-temperature spectral responses of the fabricated ZnO PD as a function of incident light wavelength, using a 300-W Xe lamp dispersed by a monochromator as the excitation source. During these measurements, the monochromatic light was calibrated with a UV-enhanced Si diode, and the optical power meter was modulated by a mechanical chopper and collimated onto the front side (i.e., metal side) of the fabricated devices using an optical fiber. The photocurrent was then recorded by a lock-in amplifier. It should be noted that photoresponses of the fabricated PD were flat in the short-wavelength region, while a cutoff wavelength was observed at around 350 nm. This indicated that the fabricated ZnO PD was indeed visible-blind. With an incident light wavelength of 350 nm and 5 V applied bias, the measured responsivities were 68.5 A/W for the film, suggesting the existence of photoconductive gain in the ZnO PD [19]. Recently, high photoconductive gain was observed from ZnO [20] and SnO₂ [21] nanowire PDs. The photoconductive gain in these oxide semiconductor nanowires was shown to be related to the molecular sensitization mechanism and/or the hole-trapping effect [20, 21]. Similar phenomena also occurred in our ZnO thin film PD prepared by the SILAR method. In the dark, oxygen molecules adsorb on the thin film surface and capture free electrons from the n-type ZnO. Therefore, a depletion layer with low conductivity is created near the surface. Under 350-nm UV irradiation, electron-hole pairs will be generated in the depletion region. The photogenerated holes oxidize the adsorbed negatively charged oxygen ions on the surface, while the remaining electrons in the conduction band increase the conductivity. These oxygen-related hole-trap states at the thin films surface prevent charge-carrier recombination and prolong the photocarrier lifetime.

Recently, *Ji et al.* reported the fabrication of a ZnO nanorod UV PD [22]. It was found that this ZnO nanorod PD can provide a higher responsivity and a larger UV-to-visible rejection ratio than does the conventional 2D ZnO PD. Comparison of their results with ours indicated that the performance of the ZnO thin film PD was not optimized. We believe that the low responsivity is related to the poor carrier collection efficiency from the electrodes, since the 0.2-mm finger spacing is too long. We should be able to achieve a much larger responsivity by optimizing the fabricated parameters of the ZnO PD. The above results nevertheless suggest that the ZnO thin films deposited by SILAR methods are potentially useful for practical applications.

4. CONCLUSIONS

In summary, we report for the first time the fabrication of a ZnO PD by SILAR involving the use of ethylene glycol. The average diameter of ZnO was around 100 nm. In addition, the obtained hexagonal ZnO thin films grew along the c-axis and with stronger intensity at the peak (002) plane; further, the films had a smooth surface morphology and showed high transparency in the visible spectral range. The fabricated ZnO PD was visible-blind with a cutoff wavelength around 350 nm. Under a 10 V applied bias, the measured dark current was 2.58 μ A and the photocurrent was 803 μ A, and hence, the responsivities were 68.5 A/W for the ZnO PD.

ACKNOWLEDGEMENTS

The authors would like to thank the National Science Council and Bureau of Energy, Ministry of Economic Affairs of Taiwan, R.O.C., for the financial support under Contract No. 101-2221-E-006-139 and 101-D0204-6, and the LED Lighting Research Center of NCKU for the assistance of device characterization. This work was also supported in part by the Center for Frontier Materials and Micro/Nano Science and Technology, the National Cheng Kung University, Taiwan, as well as by the Advanced Optoelectronic Technology Center, the National Cheng Kung University, under projects from the Ministry of Education.

Reference

1. X.D. Gao, X.M. Li, W.D. Yu, *J. Wuhan Univ. Technol.-Mat. Sci. Edit.*, 20 (2005) 23.
2. C. Vargas-Hernandez, F.N. Jimenez-Garcia, J. F. Jurado, V. HenaoGranada, *Microelectron. J.*, 39 (2008) 1349.
3. O. Lupan, S. Shishiyanu, L. Chow, T. Shishiyanu, *Thin Solid Films*, 516 (2008) 3338.
4. O.I. Lupan, S.T. Shishiyanu, T.S. Shishiyanu, *Superlattices Microstruct.*, 42 (2007) 375.
5. O. Lupan, L. Chow, S. Shishiyanu, E. Monaico, T. Shishiyanu, V.S. Ontea, B.R.Cuenya, A. Naitabdi, S. Park, A. Schulte, *Mater. Res. Bull.*, 44 (2009) 63.
6. S. Mondal, K.P. Kanta, P. Mitra, *J. Phys. Sci.*, 12 (2008) 221.
7. S.T. Shishiyanu, T.S. Shishiyanu, O.I. Lupan, *Sens. Actuator B-Chem.*, 107 (2005) 379.
8. P. Suresh Kumar, J. Sundaramurthy, D. Mangalaraj, D. Nataraj, D. Rajarathnam, M.P. Srinivasan, *J. Colloid Interface Sci.*, 363 (2011) 51.
9. X.D. Gao, X.M. Li, W.D. Yu, *Appl. Surf. Sci.*, 229 (2004) 275.
10. A.E. Jimenez-Gonzalez, P.K. Nair, *Semicond. Sci. Technol.*, 10 (1995) 1277.

11. H. Li, J. Wang, H. Liu, H. Zhang, X. Li, *J. Cryst. Growth*, 275 (2005) e943.
12. M.H. Habibia, M.K. Sardashtia, *J. Iran Chem. Soc.*, 5 (2008) 603.
13. A. Jain, P. Sagar, R.M. Mehra, *Mater. Sci.-Poland*, 25 (2007) 233.
14. H. Miyazaki, R. Mikami, A. Yamada, M. Konagai, *Jpn. J. Appl. Phys.*, 45 (2006) 2618.
15. A. Drici, G. Djeteli, G. Tchangbedji, H. Derouiche, K. Jondo, K. Napo, J.C. Bernede, S. Ouro-Djobo, M. Gbagba, *Phys. Status Solidi A-Appl. Mat.*, 201 (2004) 1528.
16. A. Yamada, H. Miyazaki, Y.I. Chiba, M. Konagai, *Thin Solid Films*, 480–481 (2005) 503.
17. S. Sun, G.S. Tompa, C. Rice, X.W. Sun, Z.S. Lee, S.C. Lien, C.W. Huang, L.C. Cheng, Z.C. Feng, *Thin Solid Films*, 516 (2008) 5571.
18. S.C. Shei, S.J. Chang, P.Y. Lee, *J. Electrochem. Soc.*, 158 (2011) H208.
19. J. A. Garrido, E. Monroy, I. Izpura, and E. Munoz, *Semicond. Sci. Technol.*, 13,(1998) 563.
20. C. Soci, A. Zhang, B. Xiang, S. A. Dayeh, D. P. R. Aplin, J. Park, X. Y. Bao, Y. H. Lo, and D. Wang, *Nano Lett.*, 7 (2007) 1003.
21. C. H. Lin, R. S. Chen, T. T. Chen, H. Y. Chen, Y. F. Chen, K. H. Chen, and L. C. Chen, *Appl. Phys. Lett.*, 93 (2008) 112115.
22. L. W. Ji, S. M. Peng, Y. K. Su, S. J. Young, C. Z. Wu, and W. B. Cheng, *Appl. Phys. Lett.*, 94 (2009) 203106.